JOURNAL OF SPACECRAFT AND ROCKETS
Vol. 41, No. 5, September–October 2004

Design and Performance of Tip-Tilt Mirror System for Solar Telescope

Kazuhide Kodeki,* Kazuhiko Fukushima,* and Masao Inoue†
Mitsubishi Electric Corporation, Amagasaki 661-8661, Japan
Toshio Kashiwase‡
Mitsubishi Electric Corporation, Kamakura 247-0065, Japan
and
Toshifumi Shimizu,§ Taro Sakao,§ Ryouhei Kano,§ Hirohisa Hara,§ Shin′ichi Nagata,§ Tsuyoshi Yoshida,¶
and Saku Tsuneta**
National Astronomical Observatory, Mitaka 181-8588, Japan

The tip-tilt mirror (TTM) system was developed for the extreme ultraviolet (XUV) Cassegrain telescope aboard the Institute of Space and Astronautical Science sounding rocket. The spatial resolution of the telescope is about 5 arcsec, whereas the rocket pointing is only controlled to be within ±0.5 deg of the target (sun) without additional stability control. To stabilize the XUV image within about 5 arcsec on the focal plane, the TTM system controls the tilt of the secondary mirror with two-axis fixed-coil magnetic actuators. The TTM system has a wide tilt angle and can drive the large secondary mirror at high frequency. The two position-sensitive detectors, one placed in the telescope and the other in the TTM mechanical structure, are used for closed-loop control of the TTM. The closed-loop control system, which has command and telemetry, is executed by the flight software on the digital signal processor. The TTM has a launch-lock mechanism to protect against launch vibrations up to about 16G. The sounding rocket was launched from the Kagoshima Space Center on 31 January 1998. The TTM worked perfectly during the flight and achieved better than the expected 5-arcsec stability on the focal plane during CCD charge-coupled device exposures.

Introduction

RECENTLY, imaging observations of the solar corona made by the soft x-ray telescope (SXT)[1] aboard the Yohkoh satellite[2] have significantly advanced our understanding of the dynamical behavior of coronal magnetic fields, their energy release, and the accompanying magnetic reconnection.[3,4] The production of velocity-sensing field map images will be the next significant step toward determining the dynamical behavior of the solar corona. Up to now, the velocity field in the direction of the glance has been measured by obtaining, with the spectroscope, the wavelength profile in the emission line where the high-temperature plasma originated. This method has the advantage of high wavelength resolution, but the observation area must be scanned for a long time to obtain two-dimensional space information, and this method is consequently not suitable for dynamic phenomena with short time spans.

We therefore developed the solar XUV (extreme ultraviolet) Doppler telescope (XDT),[5–7] the first of its type in Japan. This telescope is designed to measure, with normal incidence multilayer optics, the XUV image, and the spatially resolved velocity field of the solar corona over all aspects of the sun, using the Fe XIV 21.13 nm emission line. The XDT, which is approximately 80 cm long, employs a normal incidence Cassegrain optical system comprising a spherical primary mirror (15 cm in diameter) and a plane secondary mirror (10 cm in diameter). Each of the mirrors is coated with multilayer materials in two sectors. A back-thinned 512 × 512 pixel SITe (Scientific Imaging Technologies) charge-coupled device (CCD) is used as the focal plane device. The use of a CCD allows us to observe the solar corona with a high dynamic signal range. The spatial resolution of the XDT is about 5 arcsec, whereas the CCD's pixel size corresponds to about 5 arcsec, resulting in a good match.

The XDT was launched on the 22nd S-520 rocket, S-520CN-22. However, the S-520CN rocket's pointing accuracy can only be controlled to aim within ±0.5 deg of the target (sun) without stability control, and the rocket's rate of stability is within ±0.05 deg/s. Consequently, the XUV image on the focal plane was expected to blur as a result of the rocket's pointing disturbance. For this reason we adopted a tip-tilt mirror (TTM) system to stabilize the XUV image of the sun. Up to now, the use of the TTM has been unnecessary because observations have been made in the low disturbance environment of satellites. However, we think that the TTM is indispensable when observations of high accuracy need to be made in turbulent environments such as in a rocket.

The TTM stabilizes the XUV image on the focal plane by tilting the secondary mirror with a two-axis fixed-coil magnetic actuator. The actuator has a wide tilt angle and can drive the large secondary mirror (10 cm in diameter, weight = 300 g) with high frequency, unlike conventional piezoelectric or moving-coil-type actuators. The two position-sensitive detectors, one placed in the telescope and the other at the bottom of the TTM, are both used for the normal and local modes of the closed-loop TTM control system. This system has four control modes with automatic transition between them: zero-position mode, hold mode, low-gain mode and high-gain mode. This arrangement gives us a wide initial acquisition angle with a single control system as well as high pointing accuracy once tracking is established. The in-flight software on the digital signal processor (DSP) executes closed-loop control with a command and telemetry interface and provides the TTM control system with a fail-safe function because the TTM cannot be maintained in flight. The use of a fast processor brings the added benefits of a significant reduction

Received 15 May 2003; revision received 2 September 2003; accepted for publication 2 September 2003.

*Research Engineer, Mechatronics Division, Advanced Technology R&D Center.
†Senior Engineer, Mechatronics Division, Advanced Technology R&D Center.
‡Senior Engineer, Space Systems Division, Kamakura Works.
§Research Associate, Solar Physics Division.
¶Graduate Student, Solar Physics Division.
**Professor, Solar Physics Division.

Table 1 XUV optics design of the XDT

Parameter	Value
Weight	43.8 kg
Telescope type	Cassegrain
Primary mirror diameter	15 cm
Secondary mirror diameter	10 cm
Distance between primary and secondary mirrors	47.5 cm
Focal ratio	F/6.3
Telescope field of view	±0.55 deg
CCD field of view	44 × 44 arcmin
CCD	512 × 512 (24 μm pixel) 1 pixel = 5 arcsec

Table 2 Mechanical and electrical properties and performance of the TTM

Parameter	Value
Weight	2.2 kg (TTM-mechanism) 1.2 kg (TTM-electronics)
Size	ϕ100 × 230 mm (TTM-mechanism) 200 × 120 × 50 mm (TTM-electronics)
Electricity consumption	<18 W (at the launch-lock) <5 W (at the pointing control)
Actuator type	Fixed-coil magnetic actuator
Sun angle detector	Position-sensitive detector
Position-sensitive-detector field of view	±1.8 deg
TTM angle detector	Quadrant-diode/light-emitting diode opposing method
Pointing range	±0.5 deg
Pointing accuracy	<5 arcsec
Band width	>30 Hz
Rocket pointing accuracy	±0.5 deg

in the weight and size of the control electronics, a more flexible control system, and a shorter design and testing period. In addition, the TTM has a launch–lock mechanism to protect against launch vibrations up to 16G, which can be locked and unlocked time after time because it uses a stepping motor. Furthermore, because the S-520CN rocket only has one gyroscope and its pointing accuracy is not very high the rocket's attitude angle is also calculated by the XDT's two position-sensitive detectors.

Table 1 shows the XUV optics design of the XDT. Table 2 shows the mechanical and electrical properties and the performance of the TTM. The tip-tilt mirror is small, lightweight, has a low electricity consumption, a wide pointing range, and high pointing accuracy.

The XDT was launched by the Institute of Space and Astronautical Science (ISAS) at around midday on 31 January 1998, from the Kagoshima Space Center (KSC) located at a latitude of approximately 31° N. Observation of the solar corona was carried out for about 5 min. The TTM worked perfectly during the flight and achieved better than 5-arcsec stability on the focal plane during CCD exposures.

Overview of the Tip-Tilt Mirror System

XDT and TTM Mechanism

Figure 1 is a schematic illustration of the XDT and the TTM inside the nose cone of the S-520CN rocket. Figure 2 shows the external view of the XDT, whereas Fig. 3 shows the external view of the TTM. Figure 4 is the schematic illustration of the TTM's mechanical structure.

There are two independent optical instruments onboard: one is the XDT for observing the solar corona, and the other is the aspect telescope that monitors the attitude of the telescope with respect to the sun during flight. The XDT optics consist of a spherical primary mirror and a plane secondary mirror. A back-thinned 512 × 512 pixel SITe CCD with 24-μm pixels is used as the telescope's detector.

The aspect telescope consists of a pinhole, a secondary XUV mirror to reflect visible light, and a position-sensitive detector (PSD) as

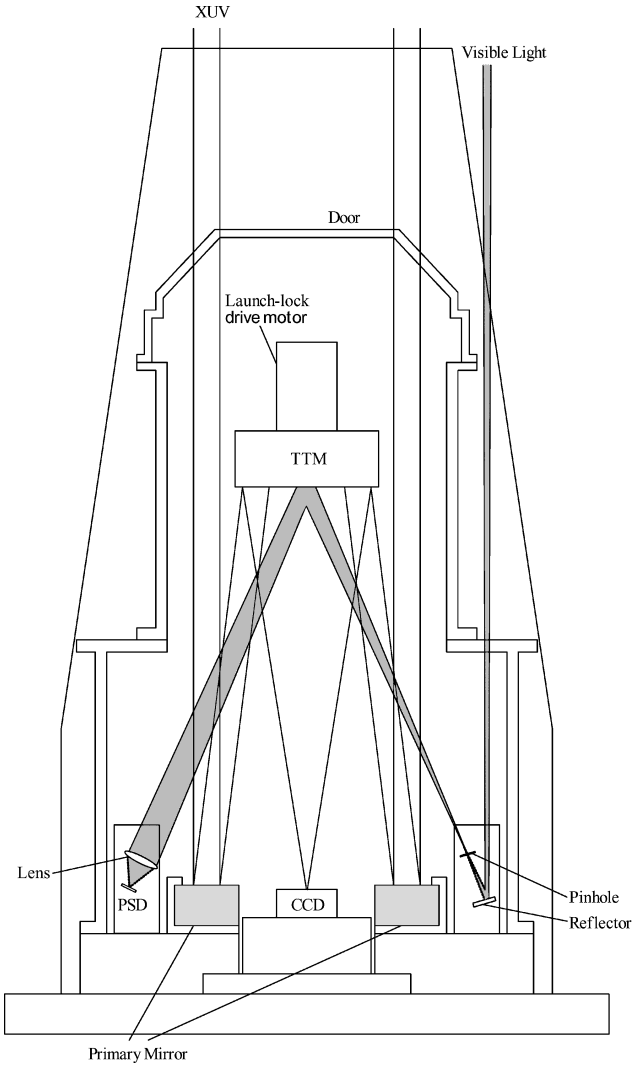

Fig. 1 Overview of XDT and TTM.

Fig. 2 XUV Doppler telescope.

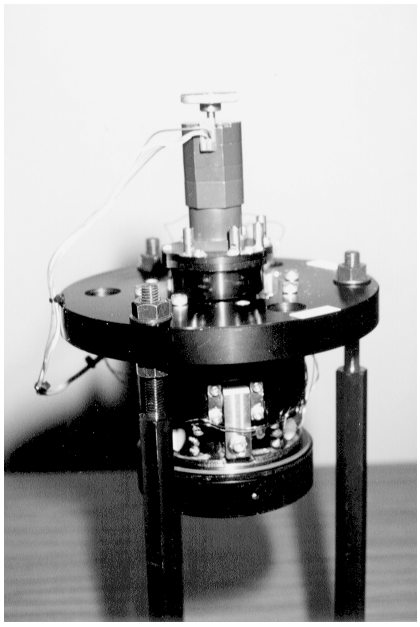

Fig. 3 Tip-tilt mirror.

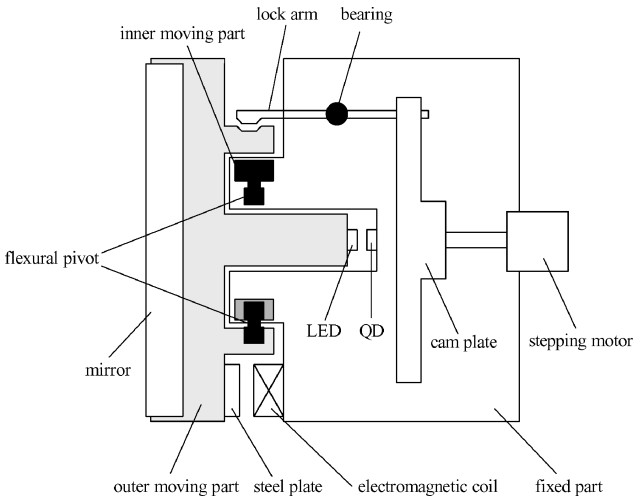

Fig. 4 TTM mechanism.

the detector. The PSD is mounted at the side of the primary mirror to sense the angle of the solar beam, and a single lens is set in front of the PSD to cover a large field of view. Another position-sensitive detector using a quadrant diode (QD) in the TTM mechanical structure senses the angle of the TTM, which is calculated by the relation between the QD attached to the fixed part of the TTM and the light-emitting diode (LED) attached to the moving part of the TTM. Angle detection accuracy with the QD and the LED is about 0.02 deg and with the PSD is about 0.2 arcsec. The zero-position mode uses only the QD; however, hold mode, low-gain mode, and high-gain mode use both the QD and the PSD. The TTM is controlled by sensing the centroid position of the visible sunlight on the PSD, as the XUV image of the sun does not move on the CCD.

The TTM's inner moving part and fixed part are connected by two flexural pivots, as are its inner and outer moving parts. This arrangement gives two degrees of freedom for rotation. Three fixed-coil magnetic actuators control the moving part of the TTM. The actuators have a wide tilt angle (±0.5 deg), and are able to drive the large secondary mirror (10 cm, 300 g) with high frequency (>30 Hz). The actuators are arranged 120 deg apart and can control rotation with two degrees of freedom. This configuration achieves a significant reduction in weight, size, and cost.

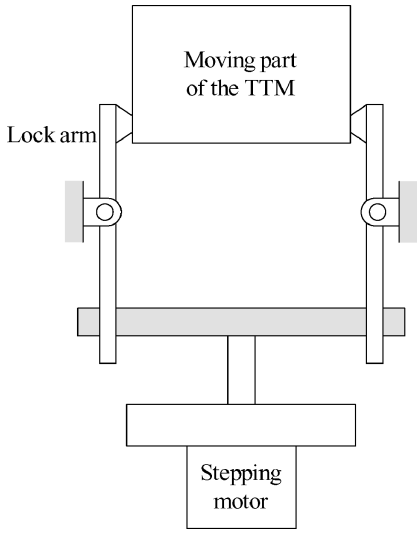

Fig. 5 Launch-lock in locked state.

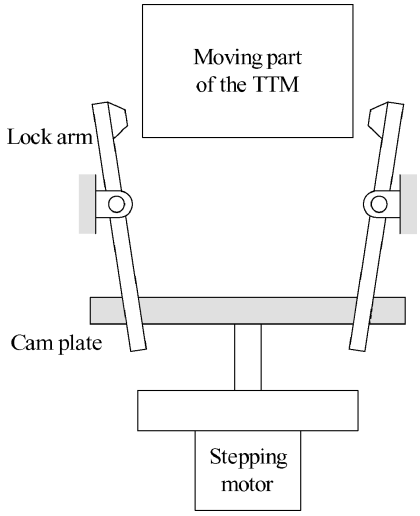

Fig. 6 Launch-lock in unlocked state.

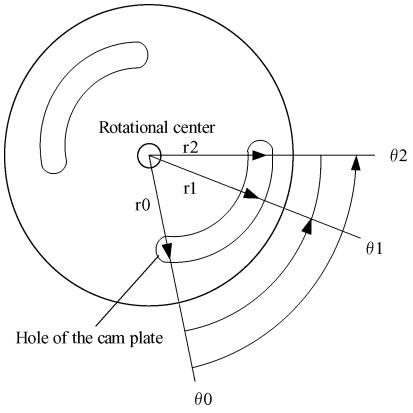

Fig. 7 Cam plate.

Launch–Lock Mechanism

The TTM has a launch–lock mechanism to protect against launch vibrations of up to 16G. Figure 5 shows the locked state, and Figure 6 shows the unlocked state of the launch–lock mechanism. Figure 7 shows the cam plate, and Fig. 8 shows the relation between the rotational angle of the cam plate and the radius of curvature. When the rotational angle of the cam plate is θ_0, the distance between the rotational center and the hole of the cam plate is shortest; thus, the radius of curvature is shortest. In this position the lock-arms release

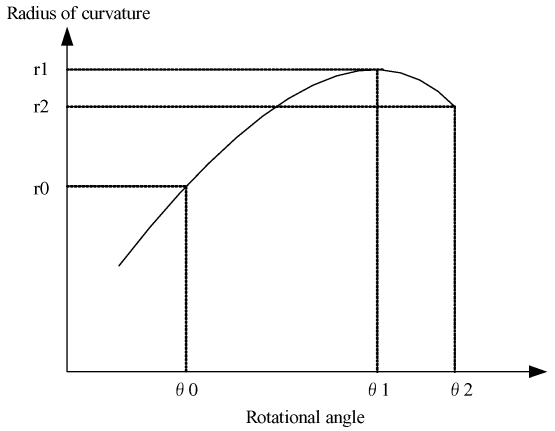

Fig. 8 Relation between rotational angle of cam plate and radius of curvature.

the moving part, and the launch-lock switches to the unlocked state. On the other hand, when the rotational angle of the cam plate is θ_2, the distance between the rotational center and the hole of the cam plate becomes longer. The radius of curvature then becomes longer than r_0, and the lock-arms catch the moving part, and the launch-lock engages to the locked state. The lock and unlock modes can be engaged time after time because the stepping motor connected to the cam plate can rotate in a clockwise or anticlockwise direction. This means that ground-based tests can also be performed repeatedly. Two limit switches are situated below the cam plate and can sense when the lock or unlock modes switch. In addition, the TTM has a fail-safe function run by software. If the limit switches are broken because of launch vibration or the stepping motor slips during flight, the TTM cannot begin to track the sun. In that case, the number of step pulses from the stepping motor is compared with the number of step pulses determined by the software. When the former is greater than the latter, the TTM will start to track the sun. A timer command initiates the release of the launch-lock mechanism after the rocket is burned out and disengages. The launch-lock operation takes about 40 s to complete.

Electronics

The various TTM control processes are performed by the TTM electronics (TTM-E) package installed in the side of the XDT body. The system uses a DSP for high-speed processing, and it is possible to change the software to suit various operation modes and various constants. Furthermore, control of the command and telemetry interface components is achieved with a field programmable gate array (FPGA). The use of the DSP and FPGA delivers a significant reduction in the weight and size of the control electronics, a more flexible control system, and a shorter design and testing period.

Design of the TTM Control System

Control Modes

The TTM has four control modes with automatic transition between them: zero-position mode, hold mode, low-gain mode, and high-gain mode. The zero-position mode is used before image acquisition, and the TTM is controlled at the zero position by local closed loop using only the QD. The hold mode is used when the rocket's aim is more than ± 0.5 deg outside the desired direction because the TTM's movable range is less than ± 0.5 deg. This mode is used to move the solar beam to the center of the CCD as quickly as possible. The low-gain mode is used in the initial image acquisition stage and when the PSD's gain is low and its field of view is wide. The high-gain mode is used in the normal tracking mode and when the PSD's gain is high and it has high resolution. This arrangement gives us a wide initial acquisition angle with a single TTM system as well as high pointing accuracy once tracking is established. The hold mode, low-gain mode, and high-gain mode use the QD and PSD to give the TTM an offset angle because the XUV telescope optics do not agree with the aspect telescope optics.

Rocket Attitude Control System

Because the S-520CN only has one gyroscope, its pointing accuracy is not very high; it is greater than 0.5 deg because of a control dead band and bias error caused by various factors. However, the TTM has a pointing range of 0.5 deg. Therefore, we employed two position-sensitive detectors (PSD and QD) to calculate the correct rocket attitude angle. If the solar beam is detected within the PSD's range, the TTM system sends the rocket the sun presence signal and the rocket attitude angle data, and the rocket is controlled using the calculated rocket attitude angle. If a solar beam is not detected by the PSD, the rocket is controlled using the gyroscope.

Design of the Control System for the High-Gain Mode

In the XDT optical system Eq. (1) represents the relationship between the output of the PSD, the sun angle disturbance, and the TTM angle:

$$\psi = \phi - B\theta$$

$$B \equiv \frac{2L_{\mathrm{PSD}}}{L_{\mathrm{PIN}} + L_{\mathrm{PSD}}} \tag{1}$$

where ψ is the output of the PSD, ϕ the sun angle disturbance, θ the TTM angle, L_{PSD} the distance between the TTM and the PSD, and L_{PIN} the distance between the pinhole and the TTM. Moreover, it is necessary to point the TTM angle to the target value, which is shown by Eq. (2), for the geostationary of the XUV image on the CCD at a fixed position with accuracy below 5 arcsec:

$$\theta = \phi/A$$

$$A \equiv (f + z_{\mathrm{CCD}})/f \tag{2}$$

where f is the focal length of the primary mirror and z_{CCD} the back focus of the CCD. The TTM can be considered to be a spring-mass system because of the use of flexural pivots. We therefore considered the proportional integral derivative (PID) control law for the TTM control system. Also, by solving Eqs. (1) and (2), we defined a target to adjust Eq. (3) to 0 in the TTM control system:

$$e = [(B - A)\theta + \psi]/A \tag{3}$$

A block diagram of the control system with the PID control law is illustrated in Fig. 9. The S-520CN rocket that launched the TTM flies at uniform velocity, and its rate of stability is ± 0.05 deg/s. In this case the pointing error of the TTM to the sun angle disturbance is given by Eq. (4), which is obtained by using the final-value theorem:

$$e/\phi = kv/Aki \tag{4}$$

where kv is the stiffness of the flexural pivot and ki the integral gain.

In the TTM system disturbance is a ramp input, and so we also considered the I-PD control law.[8] A block diagram of the control system with the I-PD control law is illustrated in Fig. 10. In this case the pointing error of the TTM to the sun angle disturbance is given by Eq. (5), which is also obtained by using the final-value theorem:

$$\frac{e}{\phi} = \frac{kv + (B - A)kp}{Akpki} \tag{5}$$

where kp is the proportional gain.

In Eqs. (4) and (5) kv is much larger than the term B-A. Therefore, the pointing error can be reduced by setting kp to a suitable value, and the pointing error for the I-PD control law is smaller than that for the PID control law.

Then, we considered the I + PID control law to improve the disturbance suppression characteristic of the TTM control system still further. A block diagram of the control system with the I + PID control law is illustrated in Fig. 11. In this case the pointing error of

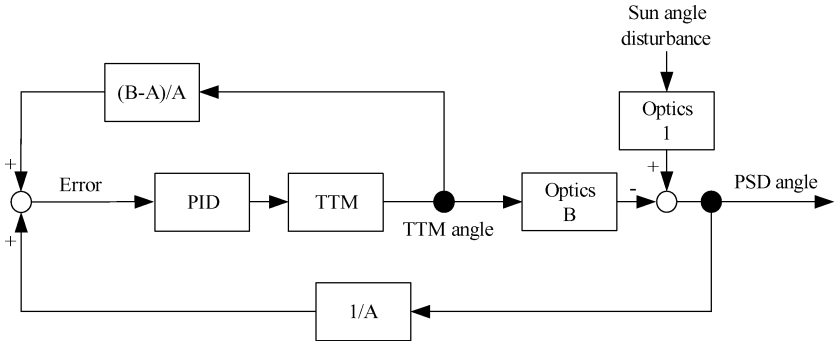

Fig. 9 Block diagram of TTM control system with PID.

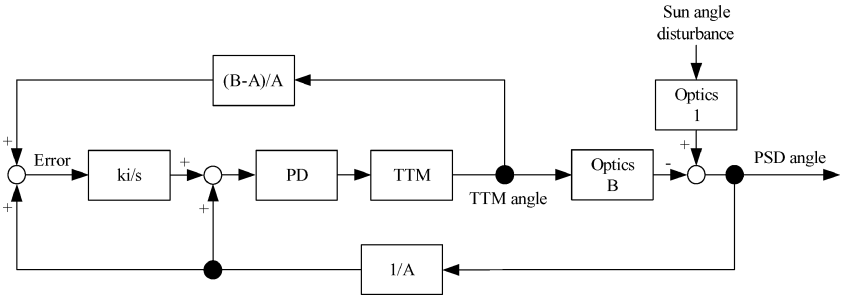

Fig. 10 Block diagram of TTM control system with I-PD.

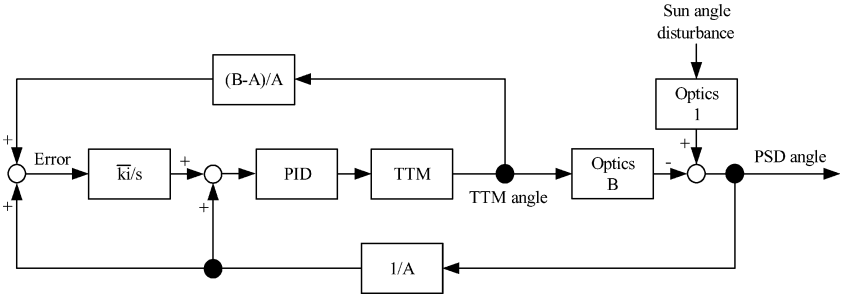

Fig. 11 Block diagram of TTM control system with I + PID.

the TTM to the sun angle disturbance is given by Eq. (6) obtained by using the final-value theorem:

$$e/\phi = (B - A)/A\overline{ki} \tag{6}$$

where $\overline{ki}$ is the additional integral gain. By assuming $\overline{ki}$ and ki to be the same value in Eqs. (5) and (6), the pointing error for I + PID control law is smaller than that for I-PD control law.

Therefore, we adopted the I + PID control law, which best reinforces the integral control of the TTM control system. We also determined the I + PID gain so that the control system had a crossover frequency of more than 30 Hz. We also had to estimate the TTM control error for the disturbance torque of the S-520CN rocket thruster, which has the characteristics shown in Fig. 12. Figure 13 shows the numerical simulation result for this disturbance torque. The result shows that the TTM control error is about 1 arcsec, well under the specified 5 arcsec. Next, we show the result of simulating the TTM response when the S-520CN rocket's attitude changes at uniform velocity. Here, we consider the worst case in which the S-520CN rocket's attitude change is 0.09 deg/s. This corresponds to a triangular wave that has an amplitude of 13 $\text{arcmin}_{\text{p-p}}$ and is 5 s of a period. Figure 14 shows the S-520CN rocket attitude, and Fig. 15 shows the TTM control error. In Fig. 15 the control error is about 4 arcsec, showing that the TTM control system has an adequate disturbance suppression characteristic. Therefore, we conclude that the sun's image on the CCD can be stabilized to within 5 arcsec and that the control system has the appropriate crossover frequency.

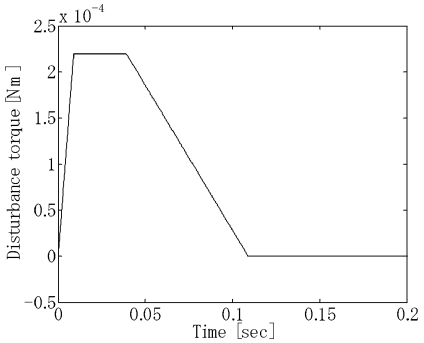

Fig. 12 TTM disturbance torque of the S-520CN rocket.

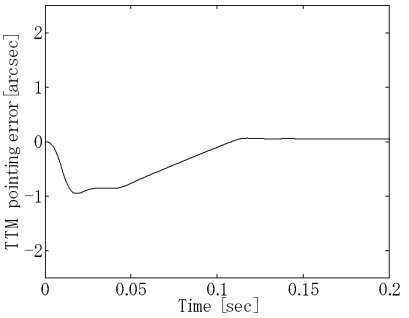

Fig. 13 Estimation of TTM control error when the S-520CN rocket thrusts as shown in Fig. 12.

Experimental Results

Performance Evaluation Examination

In this section we present the experimental results. We tested the TTM using the high-quality 2/100 solar simulator at ISAS. Another tip-tilt mirror was set in front of the TTM system to change the input beam angle in order to estimate its dynamic characteristics in conditions equivalent to those experienced in flight. We drove another tip-tilt mirror at various frequency sine waves to measure the TTM frequency response. Figure 16 shows the designed and experimental frequency responses of the TTM system's open-loop transfer function in high-gain mode. The solid line represents the designed frequency response, and the dots represent the experimental frequency response. In Fig. 16 the designed frequency response of the TTM system's open-loop transfer function agrees closely with that of the experimental frequency response. Here, the TTM system's crossover frequency is approximately 35 Hz.

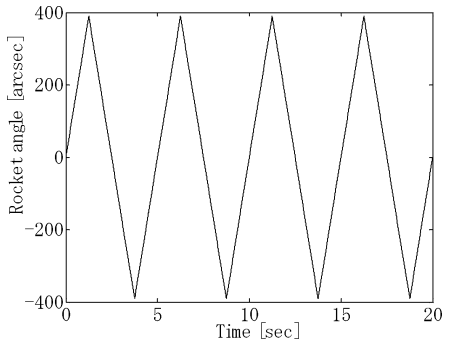

Fig. 14 S-520CN rocket attitude change.

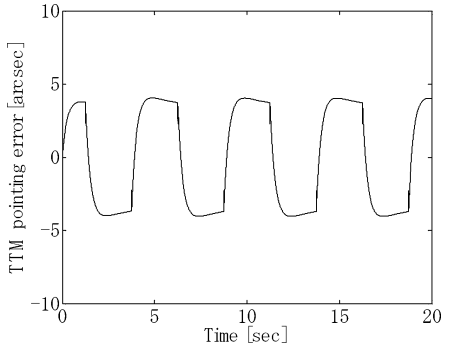

Fig. 15 Estimation of TTM control error when S-520CN rocket attitude changes as shown in Fig. 14.

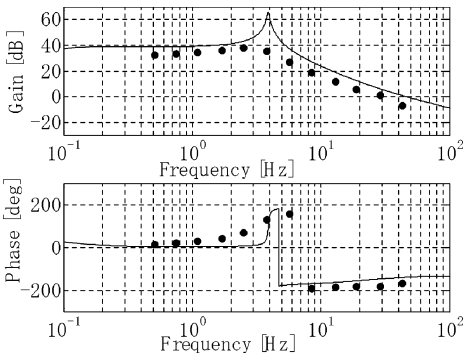

Fig. 16 Frequency responses of TTM system's open-loop transfer function in high-gain mode.

Next, we drove another tip-tilt mirror at triangular waves with a period of 5 s and an amplitude of 780 arcsec. The change rate of the input solar angle is about 0.09 deg/s and is double the predicted worst rate of stability of the S-520CN rocket. For this configuration, the attitude change of the rocket can be simulated. Figure 17 shows the TTM's experimental time response for the high-gain mode. The control error of the TTM is less than 5 arcsec, which agrees with the simulation result. The preceding results for the worst-case rocket attitude change verify that the TTM system can track and stabilize the sun's image. Figures 18 and 19 show solar images on the CCD: Fig. 18 shows the solar image when the TTM is locked mechanically and it is not operated, whereas Fig. 19 shows the solar image when it is operated in the high-gain mode. In Fig. 19 the sun image is not blurred but clear, unlike in Fig. 18. From these results it was verified that the TTM system can reduce the tracking error. In addition, we performed vibration tests up to 16G on the TTM system. After the vibration tests it was found that the system was not damaged at all and could be controlled normally.

Flight Result

The sounding rocket S-520CN-22 equipped with the XDT was launched from the KSC at 13:30 (Japan Standard Time) on 31 January 1998. The release of the launch-lock mechanism began 67 s after launch. Meanwhile, the attitude control system of the rocket, which functioned to point the telescope in the direction of the sun, was based on the gyro signal. The sun came into the PSD field of view 102 s after launch. Afterward, the rocket attitude control system was controlled based on the sun angle provided by the TTM system, and the sun angle was within the range of ± 0.3 deg. The release of the launch-lock mechanism was completed 108 s after launch, and the TTM system made the transition to the zero-position mode using the QD. The system then switched to high-gain mode using the QD and PSD 117 s after launch and began to track the sun. Then, the XUV image on the CCD was stabilized by the TTM system for about 5 min.

Figure 20 shows the change of the sun angle, whereas Fig. 21 shows the change of the sun's angle on the PSD in flight. The sun angle corresponds to the rocket attitude angle in Fig. 20. In Figs. 20 and 21 the dark areas indicate that the CCD was taking a photograph. In both of these figures, the positive direction of the south–north axis corresponds to the positive direction of the yaw angle, and the positive direction of the east–west axis corresponds to the negative direction of the pitch angle. In Fig. 21 CCD image number 1 has not been stabilized at the center by the TTM because the picture was taken in the zero-position mode, whereas the other CCD images have been properly stabilized to the center.

Figure 22 shows the time response of the sun angle in the pitch direction, whereas Fig. 23 shows the time response of the sun angle

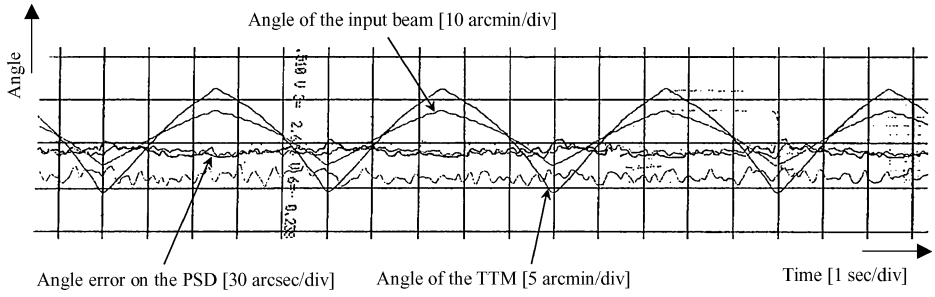

Fig. 17 Experimental time response of TTM.

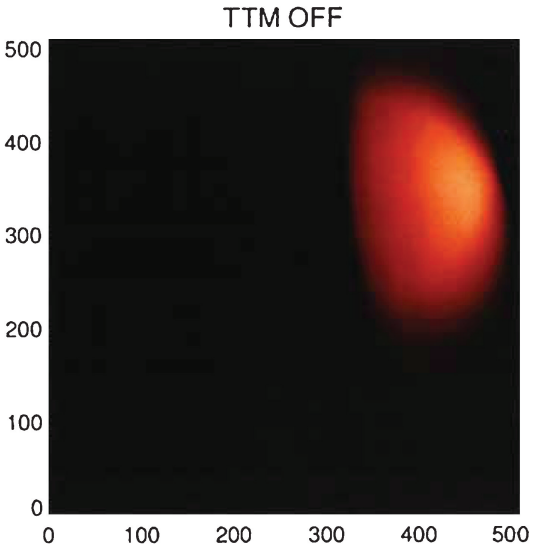

Fig. 18 Solar image when TTM is locked mechanically.

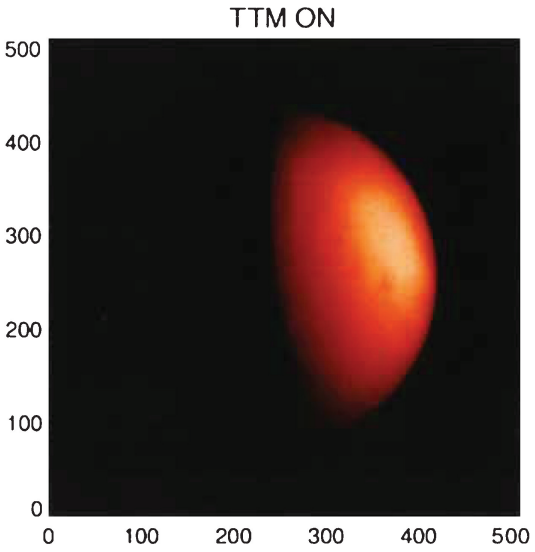

Fig. 19 Solar image when TTM is operated in high-gain mode.

in the yaw direction in flight. These figures show that the attitude of the rocket deteriorated by 0.044 deg/s within the range of ±0.3 deg. Figure 24 shows the time response of the TTM angle in the pitch direction, whereas Fig. 25 shows the time response of the TTM angle in the yaw direction in flight. Figure 26 shows the time response of the sun angle in the pitch direction on the PSD, and Fig. 27 shows the time response of the sun angle in the yaw direction on the PSD in flight. Because these angles are telemetric data for the monitor, the telemetry width of the bit has only about 20 arcsec for a target accuracy of 5 arcsec. In addition, because the TTM adjusts the sun angle on the PSD according to the TTM tilt a slight change in the sun angle on the PSD can be seen when the angle of the sun increases. Figure 28 shows the XUV image acquired by the CCD in flight. The XUV image is stabilized by the TTM system, and there is no blurring at all.

From the performance evaluations conducted on the ground, we had confirmed that the TTM's performance specifications would be able to withstand conditions twice as severe as those experienced in actual flight. Moreover, the blurring observed in the experiments and thought to be a result of resolution deterioration did not occur in the images acquired in flight. Furthermore, we compared images acquired by the XDT with images that have been acquired by the SXT. Both these telescopes have the same degree of the spatial resolution. We confirmed that deterioration in resolution was not

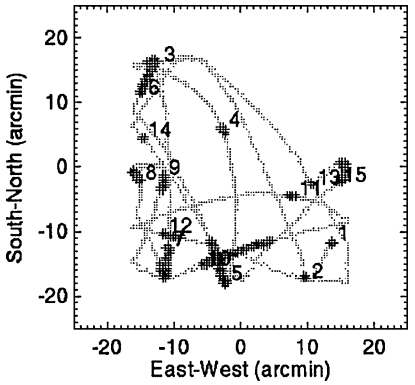

Fig. 20 Change of sun angle.

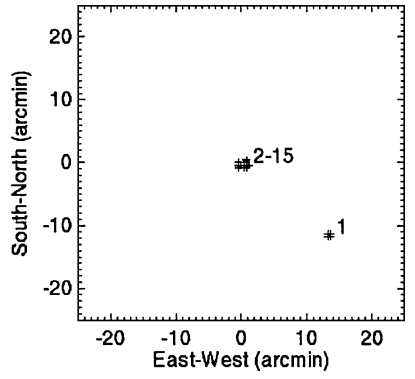

Fig. 21 Change of sun angle on PSD.

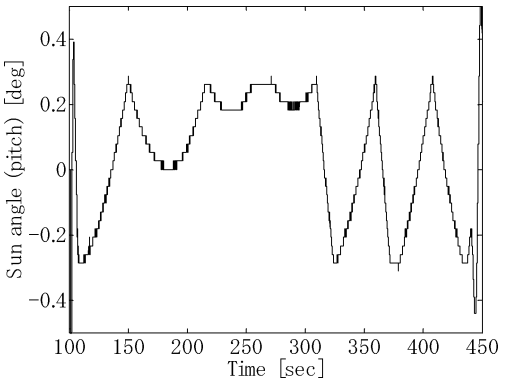

Fig. 22 Sun angle of pitch direction.

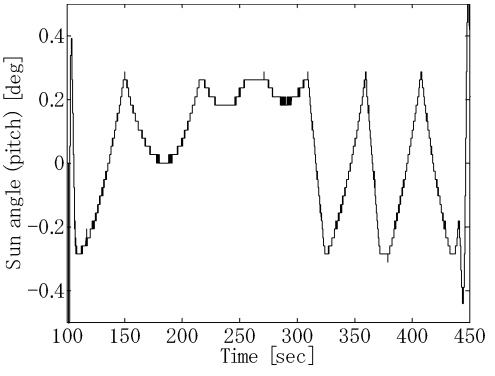

Fig. 23 Sun angle of yaw direction.

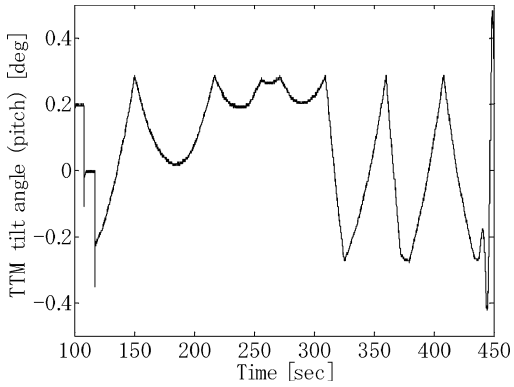

Fig. 24 TTM angle of pitch direction.

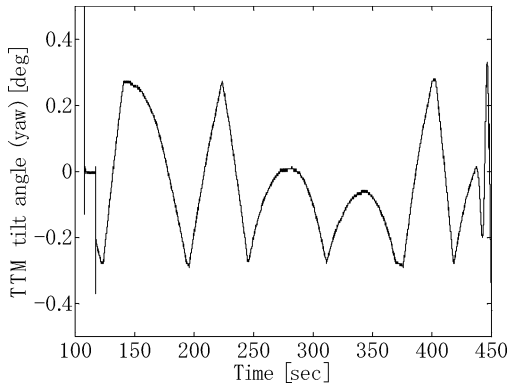

Fig. 25 TTM angle of yaw direction.

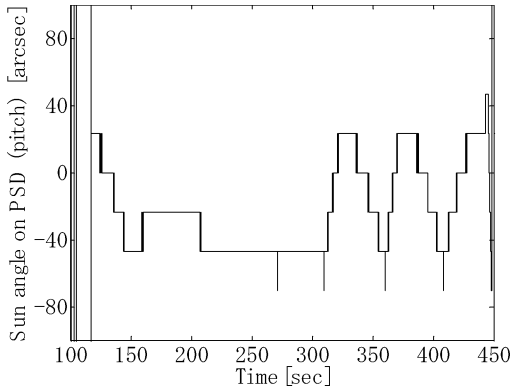

Fig. 26 Sun angle of pitch direction on PSD.

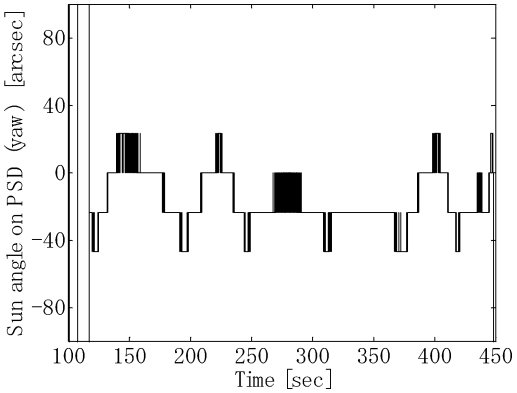

Fig. 27 Sun angle of yaw direction on PSD.

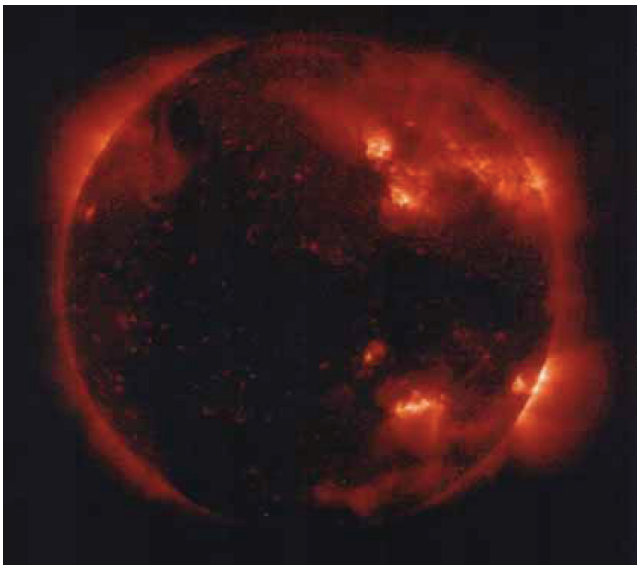

Fig. 28 XUV image in flight.

seen in images that were acquired by the XDT. Therefore, it can be concluded that the accuracy control of the XUV image projected onto the CCD had been stabilized to less than 5 arcsec while in flight.

Conclusions

In this paper we have presented the mechanism, control method, performance evaluation, and flight results of the tip-tilt mirror (TTM) system. The I + PID control law was adopted for this system because the rocket that launched the TTM flew at uniform velocity with a rate of stability of ±0.05 deg/s. The designed frequency response of the system's open-loop transfer function agreed closely with its experimental frequency response, and the crossover frequency was approximately 35 Hz. We verified that the TTM system can track and stabilize the sun's image within 5 arcsec for the worst-case rocket attitude change, which is approximately 0.09 deg/s and double the predicted worst rate of stability of the S-520CN rocket. In addition, we performed vibration tests for 16G. After the vibration tests it was found that the TTM system was not damaged at all and could be controlled normally. Finally, we verified that the accuracy control of the XUV image projected onto the CCD had been stabilized to less than 5 arcsec while in flight. The TTM system was thus proven to be effective in a turbulent environment such as in a rocket.

Acknowledgments

The authors express their sincere thanks to Y. Ogawara and I. Nakatani of the Institute of Space and Astronautical Science for their valuable support of this project.

References

[1]Tsuneta, S., Acton, L., Bruner, M., Lemen, J., Brown, W., Caravalho, R., Catura, R., Freeland, S., Jurcevich, B., Morrison, M., Ogawara, Y., Hirayama, T., and Owens, J., "The Soft X-Ray Telescope for the Solar-A Mission," *Solar Physics*, Vol. 136, No. 1, 1991, pp. 37–67.

[2]Ogawara, Y., Takano, T., Kato, T., Kosugi, T., Tsuneta, S., Watanabe, T., Kondo, I., and Uchida, Y., "The Solar-A Mission: An Overview," *Solar Physics*, Vol. 136, No. 1, 1991, pp. 1–16.

[3]Masuda, S., Kosugi, T., Hara, H., Tsuneta, S., and Ogawara, Y., "A Loop-Top Hard X-Ray Source in a Compact Solar Flare as Evidence for Magnetic Reconnection," *Nature*, Vol. 371, Oct. 1994, pp. 495–497.

[4]Tsuneta, S., "Structure and Dynamics of Magnetic Reconnection in a Solar Flare," *Astrophysical Journal*, Vol. 456, Jan. 1996, pp. 840–849.

[5]Sakao, T., Tsuneta, S., Hara, H., Kano, R., Yoshida, T., Nagata, S., Shimizu, T., Kosugi, T., Murakami, K., Wasa, W., Inoue, M., Miura, K., Taguchi, K., and Tanimoto, K., "Japanese Sounding Rocket Experiment with the Solar XUV Doppler Telescope," *Proceedings of SPIE, Missions to*

the Sun, Vol. 2804, edited by D. M. Rust, Society of Photo-Optical Instrumentation Engineers, Bellingham, WA, 1996, pp. 153–164.

[6]Hara, H., Kano, R., Nagata, S., Sakao, T., Shimizu, T., Tsuneta, S., Yoshida, T., and Kosugi, T., "XUV Doppler Telescope with Multilayer Optics," *Proceedings of SPIE, Grazing Incidence and Multilayer X-Ray Optical Systems*, Vol. 3113, edited by R. B. Hoover, Society of Photo-Optical Instrumentation Engineers, Bellingham, WA, 1997, pp. 420–429.

[7]Nagata, S., Hara, H., Sakao, T., Shimizu, T., Tsuneta, S., Yoshida, T., Ishiyama, W., Murakami, K., and Oshino, T., "Development of the Multilayer Mirrors for XUV Doppler Telescope," *Proceedings of SPIE, Grazing Incidence and Multilayer X-Ray Optical Systems*, Vol. 3113, edited by R. B. Hoover, Society of Photo-Optical Instrumentation Engineers, Bellingham, WA, 1997, pp. 193–201.

[8]Kitamori, T., "Partial Model Matching Method Conformable to Physical and Engineering Actualities," *Proceedings of IFAC Symposium on System Structure and Control*, edited by P. Horacek, International Federation of Automatic Control, Prague, 2001, pp. 141–146.

I. Boyd
Associate Editor

Color reproductions courtesy of the National Astronomical Observatory.